Surface Pressure Fluctuations in an Atmospheric Boundary Layer

Joy Schmeer, Marco Placidi and David M. Birch*
Centre for Aerodynamics & Environmental Flow, Faculty of Engineering & Physical Sciences,
University of Surrey
Guildford, Surrey
* E-mail: d.birch@surrey.ac.uk

1 INTRODUCTION

In the wind tunnel simulation of urban canyons, surface pressure measurements remain a very valuable source of information about the flow and provide one of the simplest and most reliable techniques for obtaining estimates of critical turbulence scaling parameters such as the wall shear velocity.

Surface pressures have traditionally only been measured as time-averaged quantities. However, in dispersion studies in particular, there has been much recent attention brought to the importance of peak quantities and their significance to air quality and human health [1]. As a result, there is an increasing need for the capability of making time-resolved surface pressure measurements within a wind tunnel model of a canonical urban canyon-like geometry.

Time-resolved pressure measurements in these conditions pose some particular challenges. First, the problem of physical scale and resolution: in wind tunnels, building models tend to be small. As a result, the only practical way to access the surface pressures are with lengths of hoses connecting pressure taps in the surface to pressure sensors located elsewhere. These lengths of hose inherently distort pressure signals owing to their own internal dynamics [2]. Second, there the problem of the fundamental gain-bandwidth limitation: the maximum dynamic pressures in some environmental wind tunnel tests can be below 0.2 Pa [3], representing just 0.06% of the full-scale range of even the most sensitive conventional pressure transducers.

An instrumentation suite and technique has therefore been developed address these challenges and enable surface pressure measurements to be collected in these conditions, well-resolved in both space and time.

2 METHODOLOGY

2.1 Experimental model and instrumentation

A cube with side length h = 150 mm was selected as the test model, as a canonical representation of urban topography. The five wetted faces of the cube were fitted with 100 pressure taps each, in a 10 × 10, logarithmically-spaced grid. The pressure taps were connected to 512-channel pressure scanner (Surrey Sensors Ltd. model DPS14-160P, having a full-scale range of 160 Pa and an uncertainty of 0.5%FS) by means of ~1.4m lengths of 1 mm ID hose.

The model was tested both in isolation and as an element of a staggered array of cubes with spacing 2h in the EnFlo Atmospheric Wind Tunnel at the University of Surrey, at a free-stream speed of 2.5 m/s. A model atmospheric upstream boundary layer was developed upstream using a combination of Irwin spires and surface roughness, yielding a boundary layer thickness δ = 0.9 m and roughness velocity u_τ = 0.15 m/s (estimated using the Clauser method); more details about the facility are available in [2].

2.2 Dynamic calibration

With the lengths of tubing used, the bandwidth of the pressure measurement system was limited to under 10 Hz [3]. Dynamic calibration was therefore required. A sealed chamber was placed around the cube *in situ*. One wall of the chamber was fitted with a speaker, which could be used to dynamically vary the volume of the chamber, varying the pressure by up to 16 Pa. The chamber was also fitted with a fast pressure sensor (with a bandwidth of 1000 Hz) for use as a reference.

The pressure channels were then simultaneously dynamically calibrated using a discrete Fourier reconstruction technique [4]. Sinusoidal signals at a series of discrete calibration frequencies f_0 were sent to the loudspeaker, and the signal amplitudes were adjusted by a control system to achieve the required peak-to-peak pressures on the reference sensor (as the dynamic response of the speaker system itself was unknown).

DOI 10.5258/WES/P0015

Pressure signals from each of the 500 measurement channels were then compared to the reference pressure in the Fourier domain at each f_0, and a discrete gain $G(f_0)$ and phase shift $\phi(f_0)$ obtained. Continuous functions G and ϕ could then be inferred by third-order interpolation. During measurement, a spectral decomposition of the signals was carried out by fast-Fourier transform (FFT), were rescaled and shifted by $G(f)$ and $\phi(f)$, respectively, and returned to the time domain by inverse FFT. Figure 1 demonstrates the effectiveness of the dynamic calibration process, showing its response to a white-noise pressure signal of peak-to-peak amplitude ~5% of the full-scale range P_{FS}.

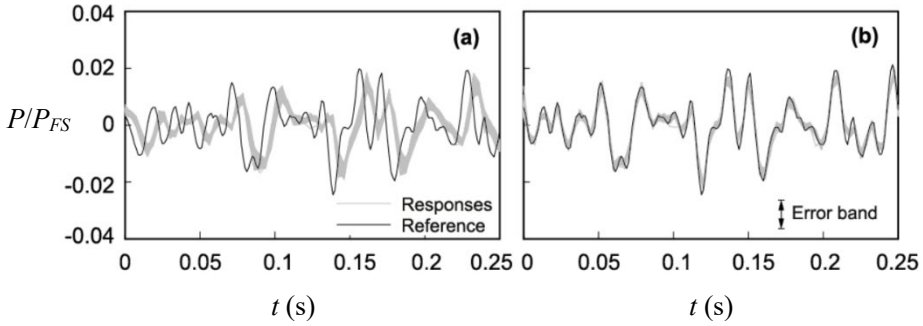

Figure 1: Effectiveness of dynamic calibration for 500 channels. (a), before calibration; (b), after.

Great care was taken to minimize the error band of pressure measurements, including temperature control, a programme of zero measurements and interpolated offsets, and simultaneous characterisation of the reference pressure. The error band reported by the sensor manufacturer is also shown in figure 1(b) as a demonstration of the improvement in sensor performance.

3 RESULTS AND DISCUSSION

3.1 Single cube

Figure 1(a) shows contour maps of the mean pressure coefficient C_P over three faces of the cube at 0º incidence for the case of the single cube in a boundary layer (note that the normalising dynamic pressure was taken at free-stream conditions). The pressure distributions agree well with a number of previously published results from both wind tunnel and field measurements.

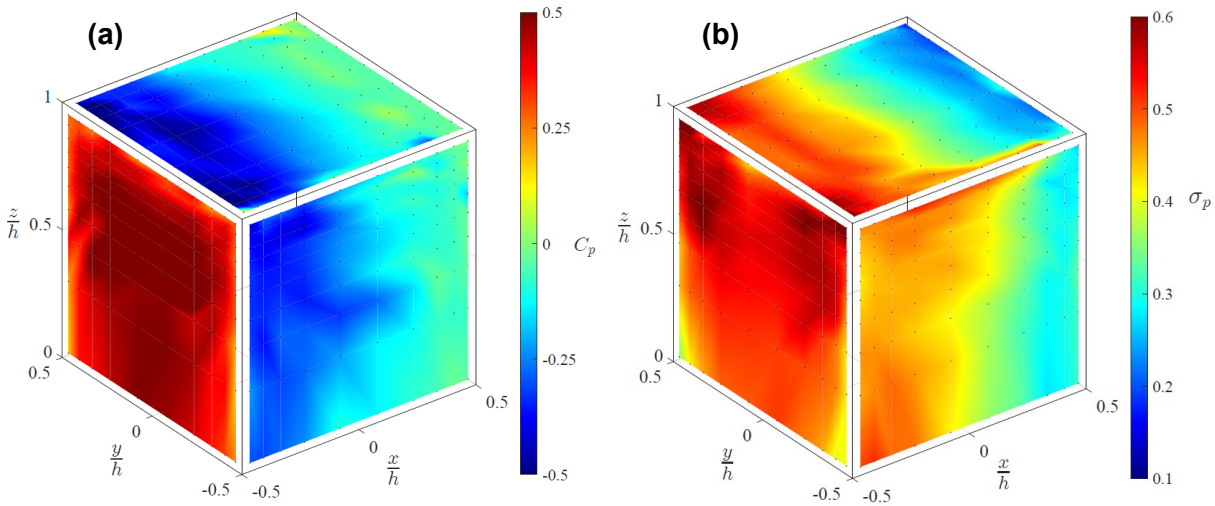

Figure 2: Resuts for a single cube in a boundary layer. (a), mean C_P; (b) standard deviation.

More interesting here, though, is figure 1(b), which shows the standard deviation σ of C_P. High levels of σ on the top corners of the leading face are consistent with the unsteadiness associated with corner vortices; likewise, at the bottom corners of the leading face there is evidence of interaction with the horseshoe vortex. Lines of high σ on the top and sides of the cube, at $x/h \sim -0.4$, are consistent with the

DOI 10.5258/WES/P0015

meandering of separation lines. A weak negative correlation in the area-averaged C_P on the two y-normal faces of the cube demonstrated that the cube could also respond to the spanwise modulation in the mean flow direction.

3.2 Staggered array

Figure 3 shows C_P and σ for the case of the cube in a staggered array at 0º incidence (with the open canyons normal to the flow direction). Although the mean pressures on the cube are substantially reduced relative to the single-cube case; this is expected, as the same free-stream speed was used and the cube was now immersed in a thick roughness sublayer. The peak standard deviation remains high by comparison; fluctuations in C_P are concentrated around the top corner of the leading edge, and are likely the result of intermittent impingement by structures shed from upstream cubes, which are unlikely to penetrate deeper into the roughness array. Interestingly, the flow incidence angle was found to have a marginal effect on the area-averaged magnitudes of σ.

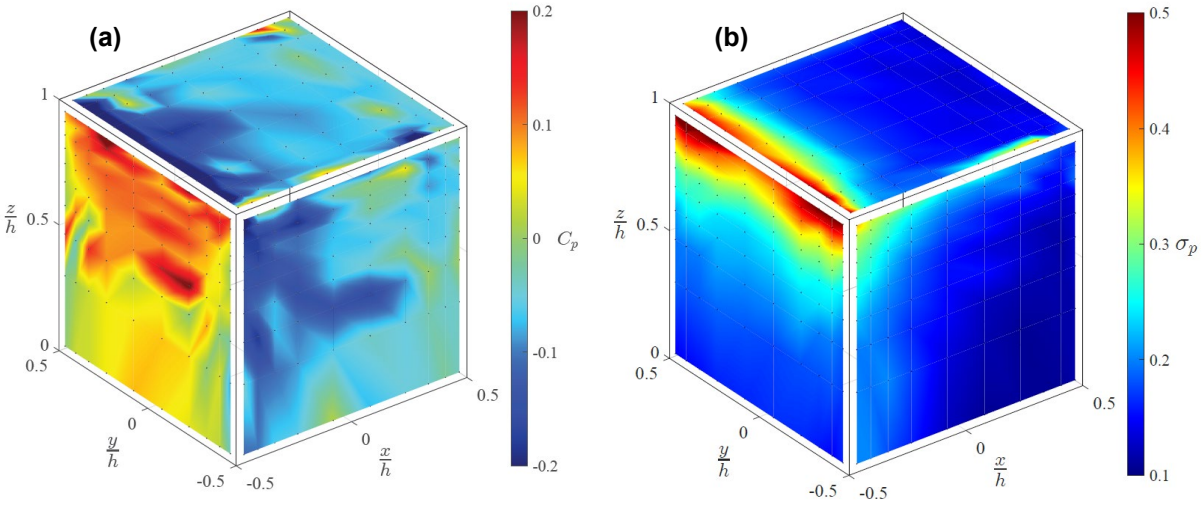

Figure 3: Resuts for a staggered cube array. (a), mean C_P; (b) standard deviation.

3.3 Friction velocity

If the pressure drag on individual roughness elements is assumed to dominate over viscous shear in the net wall shear acting on a rough surface, the shear stress acting on the cube array may be approximated as the area integral of the difference of pressures between the front and the rear faces on a typical cube, normalized by the array repeating element surface area. In the present case, the area-integral method yields a mean u_τ = 0.13 m/s, which compares well with the Clauser estimate.

With the instrumented cube, it is also possible to resolve the time-history of the zero-mean side-shear velocity v_τ, equivalent to the cross-flow wall shear. Figure 4 shows the time-histories of u_τ and v_τ, normalized against U. The streamwise component of wall shear can experience fluctuations with amplitudes as high as three times its mean value, and is indeed negative for some time (as a result of local recirculation). Note that it was assumed in these cases that $u_\tau = (\tau/\rho)^{1/2}$ was computed from the absolute value of τ but retained its sign, as the friction velocity resulting from negative shear would otherwise be undefined.

The side-shear velocity v_τ had a mean value near zero, as expected. However, the distribution was not normal; rather, it was symmetric and bimodal (with peaks at $v_\tau/U \sim \pm 0.05$; see inset). The mechanisms causing this bimodal behaviour were not clear from the evidence available; there was no significant correlation between the area-averaged pressure coefficients on the two sides of the cube (correlation coefficients in C_P were below 0.1).

DOI 10.5258/WES/P0015

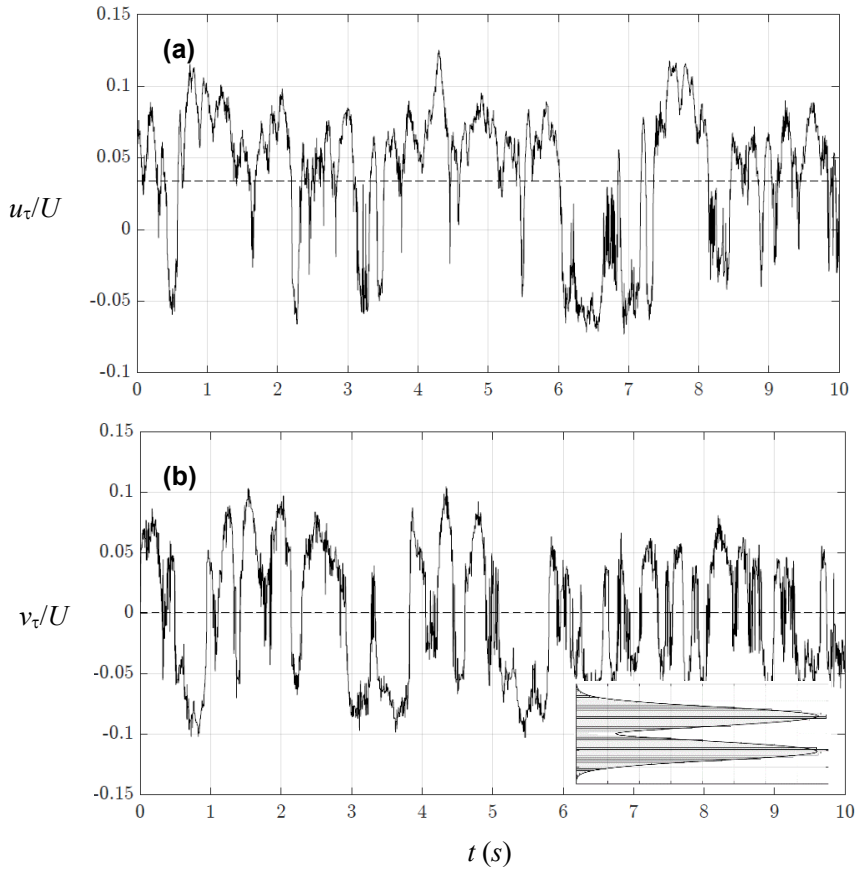

Figure 4: Time history of wall shear velocity. (a), u_τ; (b) v_τ. Inset: probability distribution of v_τ.

4 CONCLUSIONS

Surface pressure measurements were collected on a cube in a boundary layer, both for cases of the individual cube and for a cube in a staggered array commonly used as an approximation of an urban topology. A large number of measurement points and a dynamic calibration process allowed the measurements to be resolved in both space and time.

Results demonstrated that the pressure time-history is rich with information about the flow, including elements of bulk background flow behaviour, meandering of separation points and impingement of coherent structures. For the array case, a time-history of shear stress may also be inferred, demonstrating a clear bimodality in the spanwise component of shear.

REFERENCES

[1] Papp, B. Istok, B. Koren, M, Balczo, M, and Kristof, G. (2024) "Statistical assessment of the concentration fluctuations in street canyons via time-resolved wind tunnel experiments." Journal of Wind Engineering & Industrial Aerodynamics 246 (2024) 105665

[2] Marucci,D. and Carpentieri, M. (2019) “Effect of local and upwind stratification on flow and dispersion inside and above a bidimensional street canyon,” Building and Environment, vol. 156, pp. 74–88, 2019.

[3] Bergh, H. and Tijdeman, H. (1965) “Theoretical and experimental results for the dynamic response of pressure measuring systems,” Netherlands National Aerospace Laboratory, Tech. Rep. TR-F238.

[4] Stefe, M., Svete, A. and Kutin, J. (2016) “Development of dynamic pressure generator based on a loudspeaker with improved frequency characteristics,” Measurement, vol.122, pp. 212–219, 2016.

DOI 10.5258/WES/P0015